Variations in the fracture behaviour of polyethylene pipe materials induced by thermal treatments

M. R. Braga, M. Rink* and A. Pavan
Dipartimento di Chimica Industriale e Ingegneria Chimica, Politecnico di Milano, Piazza Leonardo da Vinci 32, 20133 Milano, Italy
(Received 23 June 1990; revised 5 December 1990; accepted 7 December 1990)

The effect of thermal treatments on fracture behaviour of commercial pipe-grade high density polyethylenes was studied. Fracture resistance curves, i.e. fracture toughness *versus* crack growth curves, were experimentally constructed at −60°C and 23°C and the parameters characterizing fracture initiation and propagation were determined. In addition, a qualitative fracture surface analysis was carried out. Fracture behaviour appears to be complex rather than simply related to the more prominent structural features affected by thermal treatment.

(Keywords: fracture; thermal treatment; polyethylene)

INTRODUCTION

Despite its simple molecular structure, polyethylene behaviour varies depending on the supermolecular structural arrangement achieved in the crystalline state. In order to obtain the performance required in many technical applications, it would be desirable to control all variables influencing the material's structure, thus contributing to properties. In fact, it is well known that polyethylene can develop different structural patterns, from spherulitic to less organized morphologies, and form crystallites of different sizes simply by varying crystallization conditions or molecular weight[1,2]. There has been much research on this, in which both isothermal and rapid crystallization experiments have been considered[3–13].

A few authors have concentrated the analysis of experimental data on the relationship between properties and morphology. For example, Mandelkern[4] has found systematic changes in morphology by varying molecular weight and cooling rate while Ohlberg[14] has related fracture properties of thin films to spherulite size by varying molecular weight. When large thicknesses of commercial pipe-grade polyethylenes were examined, significant discrepancies were found[15,16]. Although the effects of cooling history on morphology were intensively studied, the key structural variable affecting the properties was not clearly identified[16]. The degree of crystallinity is, of course, the first characteristic one would expect to control quantitatively the macroscopic properties of the material. Other important variables that were shown to be very influential were: 'the structure of the residual amorphous region, governed to a large extent by the molecular weight; the crystallite thickness and its distribution; the relative amount and structure of the interface; the details of the crystallite or lamellar structure; the supermolecular structure'[1]. Regarding toughness, Lustiger and Markham[17] have drawn attention to the role that amorphous entangled tie molecules may play in the fracture process, and have identified the most important structural parameters controlling the concentration of tie molecules; they include molecular weight, comonomer content, degree of crystallinity, and lamellar orientation.

Most of the structural variables are dependent on the operating conditions adopted when the material is processed. In pipe manufacturing, the thermal history applied can be expected to be very influential.

In this work, the fracture behaviour of two high-density polyethylenes (HDPE) for gas piping was studied as a function of cooling history and testing temperature. Toughness was characterized by means of the J-integral method, applied following the multispecimen procedure, so as to determine the value of toughness at fracture initiation, J_{IC}, together with the entire fracture resistance J_R curve relating toughness to crack growth. A qualitative fracture surface analysis was also performed.

EXPERIMENTAL

Materials and specimens

The polyethylenes used in this work, coded M1 and M2, were commercial products containing carbon black and supplied in the form of pellets (*Table 1*).

The materials were compression-moulded into plaques 1 cm thick according to ASTM 1928-D. Plaques of 2 cm thickness were obtained by welding pairs of 1 cm plaques (the welding operation was carried out simultaneously with the thermal treatments, to be described shortly).

Bars of dimensions 20 mm × 20 mm × 127 mm, used as single-edge notch specimens (*Figure 1a*) for fracture tests, were machined from these plaques. Notching was performed in two steps: first a cut of 9 mm depth was made with a disc saw, and then an additional 1 mm was milled with a sharp V-blade, so as to obtain a notch length (a) to specimen width (W) ratio of 0.5.

* To whom correspondence should be addressed

0032-3861/91/173152-10

Thermal treatments

Welding and thermal treatments were done in one operation.Two 1 cm plaques were put in a tightly closed mould, kept at 155°C (i.e. above melting temperature) for at least 20 min and then cooled to room temperature. Different cooling paths of the general pattern shown in *Figure 2* were considered: besides slow cooling (according to ASTM 1928-D) and quenching in an ice and water mixture, a series of isothermal crystallizations were conducted at significant temperatures, followed by either slow cooling or quenching. The actual thermal histories obtained by recording the temperature with a thermocouple inserted in the core of the plaques, are given in *Table 2*.

The treated materials will be identified by adding the treatment number to the material code.

Microscopy

Scanning electron micrograph (SEM) analysis on fracture surfaces was carried out at Genoa University.

Calorimetry

Differential scanning calorimetry (d.s.c.) measurements were carried out by means of a Mettler TA 3000 calorimeter at a scanning rate of 20 K min^{-1}. The degree of crystallinity was calculated from the measured heat of fusion and the value of the pure crystal fusion enthalpy given by Mandelkern *et al.*[18]. The influence of the scanning rate was also checked.

Densitometry

Density measurements were carried out in an isopropanol–water gradient column at 23°C. Degrees of crystallinity were calculated using Chiang and Flory's relationship[19], taking due account of the presence of carbon black.

Table 1 Details of polyethylenes studied

Code	Producer and trade name	Density (g cm^{-3}) $T = 23$ C	Melt flow index (g per 10 min) 2.16 kg	5 kg
M1	Hoechst GM5010T2	0.9568	0.6	0.40
M2	DuPont SCLAIR 35 B	0.9521		0.25

Table 2 Thermal histories of the materials

Treatment no.	Step 1 T_1 (°C)	Step 1 t_1 (min)	Step 2 T_2 (°C)	Step 2 t_2 (°C h^{-1})	Step 3 T_3 (°C)	Step 3 t_3 (min)	Step 4 T_4 (°C)	Step 4 t_4 (°C h^{-1})
0	155	20	124	5	124	39	23	5
1	155	20	122.5	34	122.5	18	23	6
2	155	20	129	16	129	40	23	370
3	155	20					23	370
4	155	20	126	1	126	4320	23	370
5	155	20	123.5	1	123.5	5680	23	370
6	155	20	123.5	5	123.5	25	23	370
7	155	20	121.5	5	121.5	4320	23	370

Fracture tests

For fracture characterization, the J-integral method was adopted; this method is used for tough polymers. Size requirements are in fact satisfied by smaller specimens than those necessary in linear elastic fracture

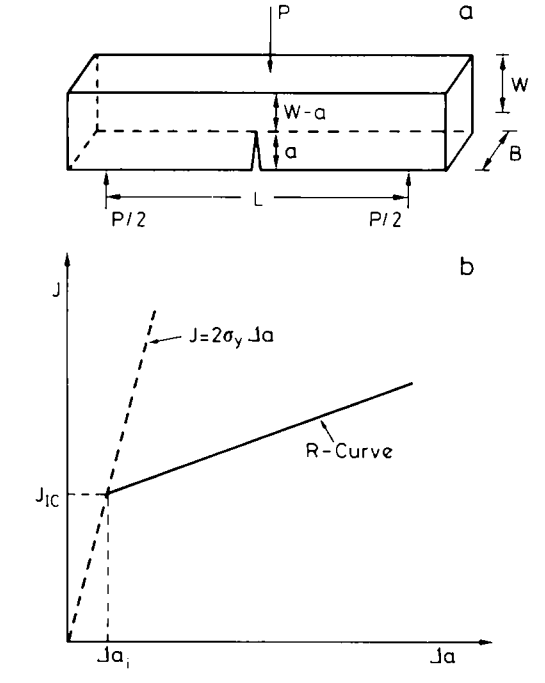

Figure 1 (a) Single-edge notch bend configuration adopted for fracture tests; (b) schematic J_R curve

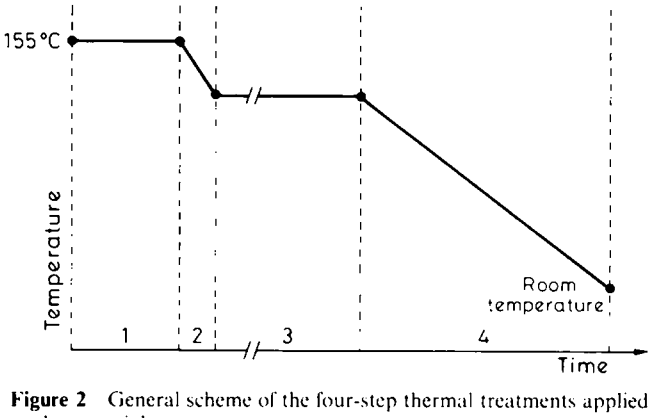

Figure 2 General scheme of the four-step thermal treatments applied to the materials

mechanics (LEFM) tests[20]. Tests were carried out in the single-edge notch bend configuration (see *Figure 1a*) with a span to width ratio, $L/W = 4$.

The procedure to determine the J_R curve is described in the literature[21,22] and has been applied to polyethylene before[23].

We determined the J-resistance curve according to the multispecimen technique (ASTM E813-81). Each of several specimens is loaded to a different deflection and J is calculated from the input energy U, measured at the final deflection according to the following equation:

$$J = \frac{2U}{B(W - a)} \quad (1)$$

in which B, W and a are specimen thickness, width and initial notch length respectively. Each specimen is then brought to complete fracture in order to observe and measure crack extension Δa. Since the crack front has a thumbnail shape, Δa was read at the furthest extension point.

J values calculated from equation (1) are then plotted against the measured Δa yielding the J_R curve. With ductile materials some crack tip blunting occurs prior to the real crack propagation, so in order to determine the initiation point, the J *versus* Δa curve is extrapolated to intersect the blunting line, which is assumed to be given by:

$$J = 2\sigma_y \Delta a \quad (2)$$

in which σ_y is the tensile yield stress. The intersection gives the J value and the apparent crack growth at initiation, J_{IC} and Δa_i respectively. Δa_i, i.e. the maximum apparent crack growth due to blunting, can be considered as a measure of the material ductility. The slope dJ/da of the linear region of the J_R curve represents the crack propagation resistance (*Figure 1b*).

J_{IC} values are deemed valid if specimen dimensions satisfy the following requirements:

$$a, W - a, B > 25J_{IC}/\sigma_y \quad (3)$$

Although the data handling recommended by ASTM E813-81 is now being questioned on the grounds that a plot of J *versus* crack extension may be non-linear for some materials, we have adopted this conventional method to identify an 'engineering' value of J at the onset of crack extension.

In the present investigation, all tests were carried out at a crosshead speed of 5 mm min^{-1} by means of an Instron testing machine, at -60°C and 23°C. Low temperature tests were carried out in an insulated box controlled by a Eurotherm unit, using CO_2 as the cooling medium. To reach thermal equilibrium at -60°C, each specimen was kept at this temperature for 45 min before measurement[24].

Tensile yield stress was determined at the same temperature using dumb-bell specimens, strained at a crosshead speed of 5 mm min^{-1}.

Crack extension evaluation

Three different procedures for surveying Δa were followed, depending on the fracture behaviour displayed by each individual specimen.

With a first group of specimens (*Figure 3a*) crack opening of the test piece before unloading was sufficient for applying an aqueous white paint down to the crack tip, by means of a very thin brush.

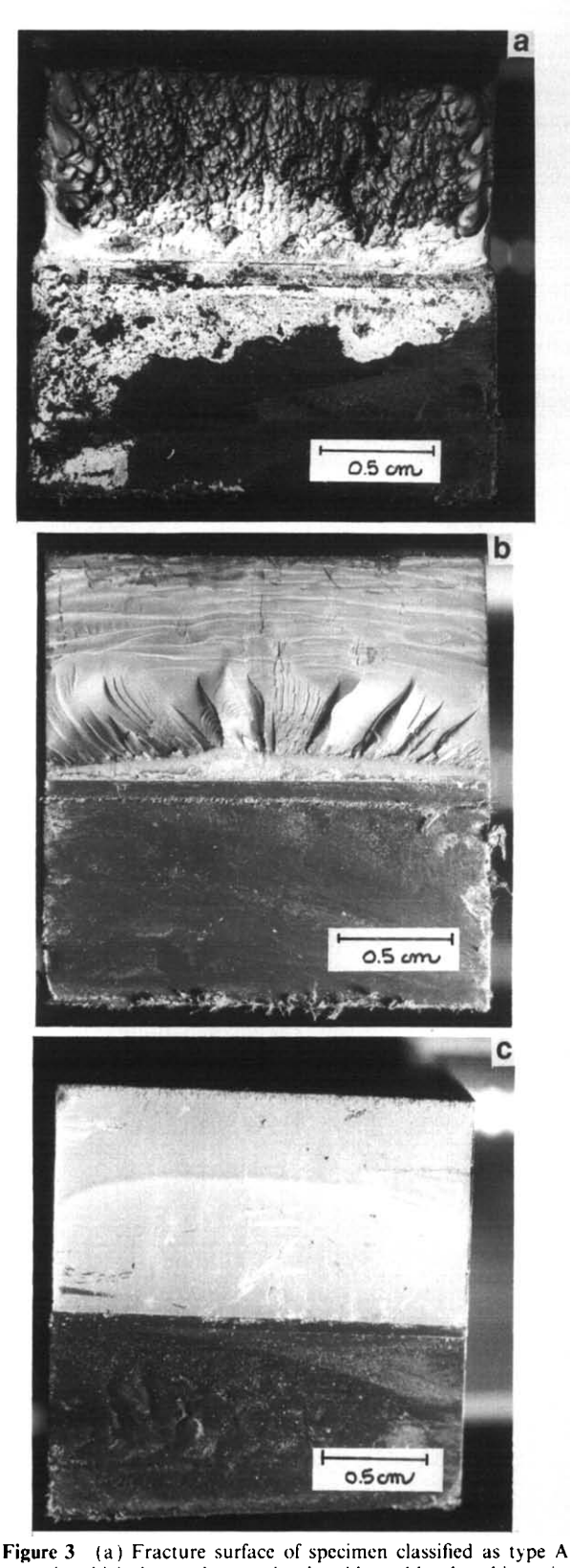

Figure 3 (a) Fracture surface of specimen classified as type A (see text), in which the crack extension is evidenced by the white paint (Δa 3.8 mm); (b) fracture surface of specimens classified as type C (see text), with crack growth extending over a limited zone beyond the machined notch (Δa 1.5 mm); (c) fracture surface of specimens classified as type B (see text), showing a well defined front trace (Δa 8.6 mm)

With a second group of specimens, however, the paint used in the previous case could not be applied, because of the narrower crack tip opening reached during the loading phase. Fracture surfaces of these specimens after

final breakage showed a well defined, flat, thumbnail-shaped area, followed by a rough zone (*Figure 3b*). In a first attempt, the crack extension was identified with the flat area on this assumption; however, meaningless J_R curves with a negative intersect at $\Delta a = 0$ were obtained. A similar outcome was observed by Melve[24], thus increasing suspicion of a misleading crack extension measurement. We therefore tried an alternative method: after unloading, the specimen was immersed in a very fluid aqueous paint exhibiting fluorescence when illuminated by a Wood lamp, allowed to dry, and then completely broken. It was observed that the actual crack extended over a rather limited zone beyond the machined notch. Significant J_R curves were obtained in this way.

With a third group of specimens, use of paint was not necessary: the fracture surface after final breakage was smooth, showing a well defined front trace (*Figure 3c*). On some of these specimens, measurement of the crack extension was confirmed by means of fluorescent paint.

RESULTS AND DISCUSSION

Thermodynamic properties

Table 3 gives data obtained from d.s.c. and density measurements. Although the thermal treatment was varied substantially, the range of crystallinity obtained varies only between 60 and 72%; generally, the lowest values correspond to rapid cooling, and the highest ones to more isothermal treatment.

It is worth mentioning that replicating the thermal treatment experiments yielded fairly reproducible results, with the exception of thermal treatment no. 6 which gave substantially different results on each of the three times it was reproduced. These are presented with the notation 6, 6 bis, 6 tris.

The degree of crystallinity obtained from density and the degree of crystallinity determined from fusion enthalpy are close to a 1:1 relationship. Both crystallinity measurements may obviously be influenced by material heterogeneity, but d.s.c. measurements are also strongly affected by the scanning-rate-dependent reorganization of the material during the scan. As it turned out from experiments not reported here, this dependence is different for differently-treated materials. Crystallinity data obtained from density measurements will therefore be considered here.

It should be noted that d.s.c. traces have sometimes presented multiple melting endotherms, which is not uncommon with polymers[25]. In *Table 3* only the peak temperature of the main endotherm is shown.

For all the thermally-treated materials, J_R curves were obtained at -60 C and 23 C, using the procedure outlined above. Fracture results are given in *Table 4*, together with yield stress, σ_y. The last column of *Table 4* gives the minimum dimension to validate the data according to the size requirements given in equation (3). Comparison with the specimen dimensions used shows that such requirements are not always met: when this occurs, the J and dJ/da values obtained are not intrinsic values, but will nevertheless be considered for purposes of comparison between the materials.

Three distinct factors affecting fracture behaviour have emerged: (1) thermal treatment, the effect of which is best observed by considering a single material tested at a single temperature (*Figure 4*); (2) type of material, the

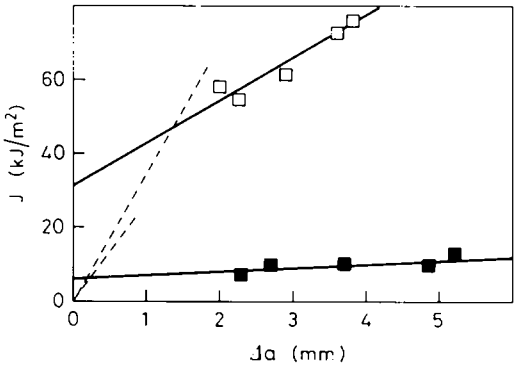

Figure 4 Effect of the thermal treatment on J_R curves: ■, treatment no. 0; □, treatment no. 1 (material M1; test temperature 23 C)

Table 3 D.s.c. and density data

Material	Thermal treatment no.	Density (g cm^{-3})	Fusion enthalpy (kcal g^{-1})	Degree of crystallinity (%) (from density)	Degree of crystallinity (%) (from d.s.c.)	T_m (C)
M1	0	0.9582	206	66.6	73.2	139.9
	1	0.9585	186	66.8	66.1	138.5
	2	0.9533	176	63.4	62.6	131.1
	3	0.9530	182	63.2	64.5	137.2
	5	0.9572	194	65.9	68.9	138.5
	6	0.9523	175	62.8	62.2	134
	6 bis	0.9555	198	64.8	70.4	133
	6 tris	–[a]	192	–[a]	68.2	135
M2	0	0.9577	187	66.3	66.5	139.3
	1	0.9578	192	66.3	68.2	142
	2	0.9511	175	62.0	62.2	136
	3	0.9507	178	61.7	63.3	133.3
	6 bis	0.9518	177	62.5	62.9	133.5
	7	0.9585	187	66.8	66.5	143

[a]Not determined

Table 4 Results of yield and fracture tests

Material and thermal treatment	Test temperature (°C)	σ_y (MPa)	J_{IC} (kJ m^{-2})	dJ/da (kJ m^{-3})	$25J_{IC}/\sigma_y$ (mm)
M1-0		16.6	47.2	11.5	71
M1-1		19.6	6.2	1	8
M1-2		16.2	60	6	70
M1-3		17.3	57	13.3	83
M1-4	23	20.1	6.4	2.6	8
M1-5		19.7	4.3	1	6
M1-6		-[a]	26	15.2	39
M1-6 bis		16.2	-[a]	-[a]	-[a]
M1-6 tris		-[a]	-[a]	-[a]	-[a]
M1-0		38	5.3	2	4
M1-1		41.7	1.9	0.2	1
M1-3	−60	55.2	16	2.5	7
M1-6 bis		50.2	9	1.2	5
M1-6 tris		-[a]	14	0.5	-[a]
M2-0		20.1	3.1	0.9	4
M2-1		19.9	4	1.5	3
M2-2		16	79	21.5	123
M2-3	23	17.1	81	17.5	118
M2-6 bis		15.8	-[a]	-[a]	-[a]
M2-7		19.8	3.4	0.6	4
M2-0		21.6	1.57	1.2	2
M2-1		19.9	1.1	1.3	1.4
M2-3	−60	35	40	2.4	29
M2-6 bis		43.9	28	1.1	16

[a]Not determined

effect of which can be seen by comparing the behaviour of the materials M1 and M2 subjected to the same thermal treatment and tested at the same temperature (*Figure 5*); and (3) test temperature, the effect of which on one material subjected to a given thermal treatment is shown in *Figure 6*.

In the first two cases, the structural features of the samples compared are evidently different, while in the third case the role these features play at different test temperatures is shown.

Fracture properties can be expected to be governed primarily by the degree of crystallinity, even though this parameter is just one of the many that characterize the semicrystalline state. In a study on commercial polyethylenes, Mandell *et al.*[15] found a unique correlation between fracture toughness K_{IC} and the degree of crystallinity when the latter is varied by changing either thermal treatment, chemical composition or molecular weight.

The degree of crystallinity is thus the first structural variable that we considered to be related to fracture properties at the two temperatures examined. The results presented in *Figure 7a* show a fairly good correlation between fracture resistance at initiation, J_{IC}, at −60°C, and the degree of crystallinity, which appears to be in agreement with the findings of Mandell *et al.* quoted above. However, no well-defined trend appears at 23°C (*Figure 8a*). If, for example, we compare the results obtained on material M1 treated following thermal treatments nos 0 and 1, although the two samples present

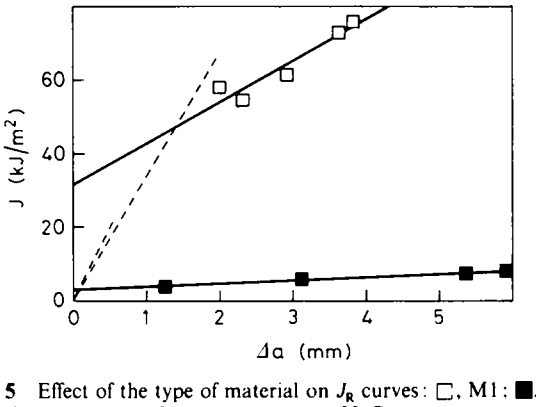

Figure 5 Effect of the type of material on J_R curves: □, M1; ■, M2 (thermal treatment no. 0; test temperature 23 C)

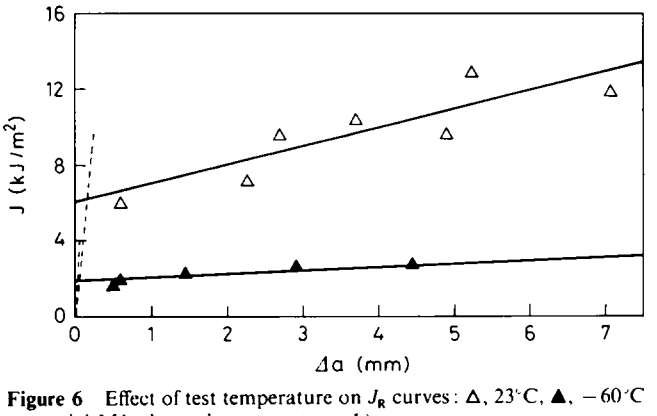

Figure 6 Effect of test temperature on J_R curves: Δ, 23°C, ▲, −60°C (material M1, thermal treatment no. 1)

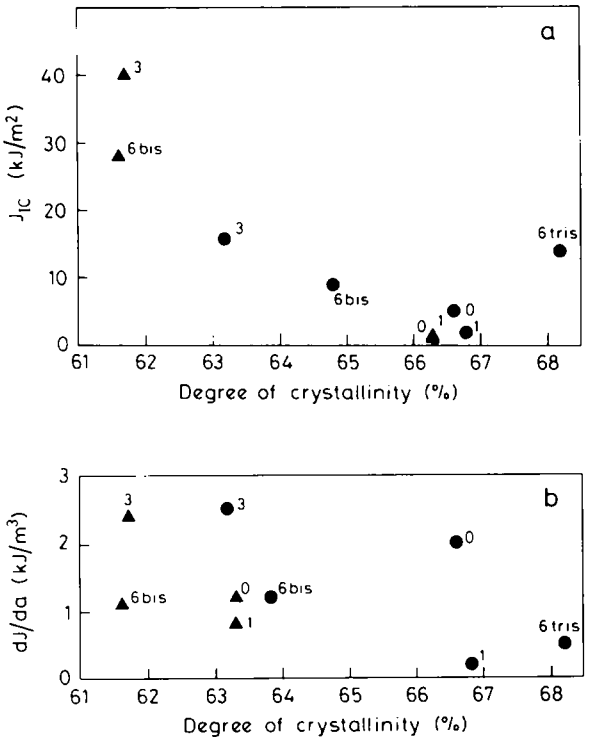

Figure 7 (a) J_{IC} and (b) dJ/da at -60°C *versus* the degree of crystallinity. ●, M1; ▲, M2. Numbers indicate thermal treatment

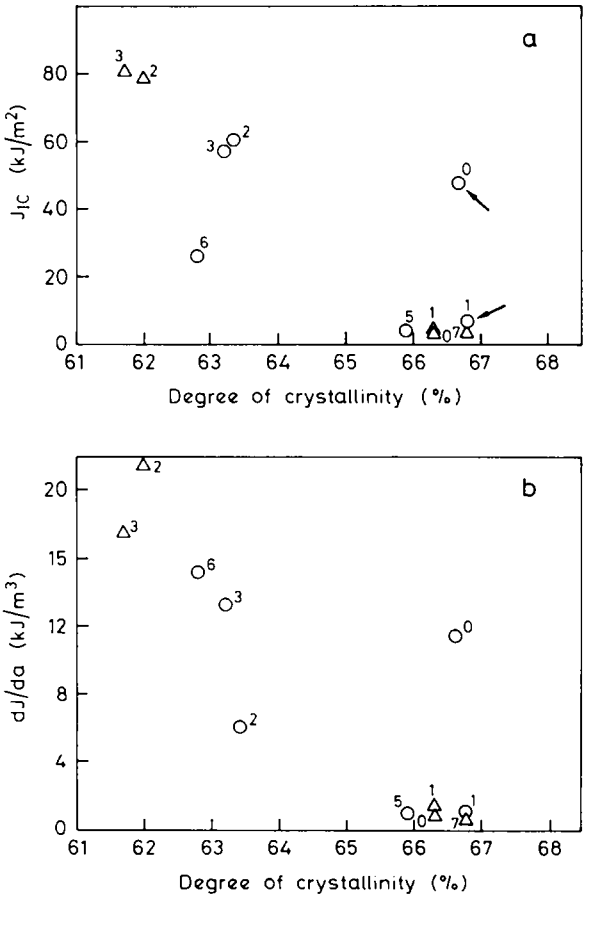

Figure 8 (a) J_{IC} and (b) dJ/da at 23 °C *versus* the degree of crystallinity. ○, M1; △, M2. Numbers indicate thermal treatment. Arrows in (a) point to the example considered in the text

the same degree of crystallinity of about 66.7%, we observe markedly different J_{IC} values, i.e. 47.2 kJ m^{-2} and 6.2 kJ m^{-2} respectively (see the two points indicated by arrows in *Figure 8a*).

It is worth observing that all specimens fractured in a barely ductile manner at -60 °C, as indicated by the low values of the resistance to crack propagation, dJ/da, in *Figure 7b*. At 23 °C, on the other hand, the values of dJ/da cover a wide range, indicating varying fracture behaviour, but without any very regular trend (*Figure 8b*).

A more direct comparison of the results obtained at -60 °C and 23 °C is given in *Figure 9*. It may be noted that the samples can be grouped into two classes according to the size of the change in the fracture resistance, J_{IC}, corresponding to the change in temperature from -60 °C to 23 °C. One class (including M1-3, M1-0, M2-3) shows a substantial variation while the second class (including M1-1, M2-1, M2-0) shows slight or no change.

Evidently the degree of crystallinity is not the only parameter that controls fracture behaviour: other features must be considered. For example, other authors[16] looked for a correlation between the heights of the secondary melting peaks in d.s.c. traces and some material properties of variously treated pipe-grade polyethylenes, but without success. Neither did they establish any link between mechanical properties and spherulite size or density, and suggested that lamellar thickness could be another significant factor to consider. In order to ascertain crystallization conditions and investigate more deeply the structural features of our samples, a further study is in progress at the University of Reading, UK and will be reported in a separate paper.

Fractographic analysis

The fracture behaviour of the materials was also investigated from the fractographic point of view.

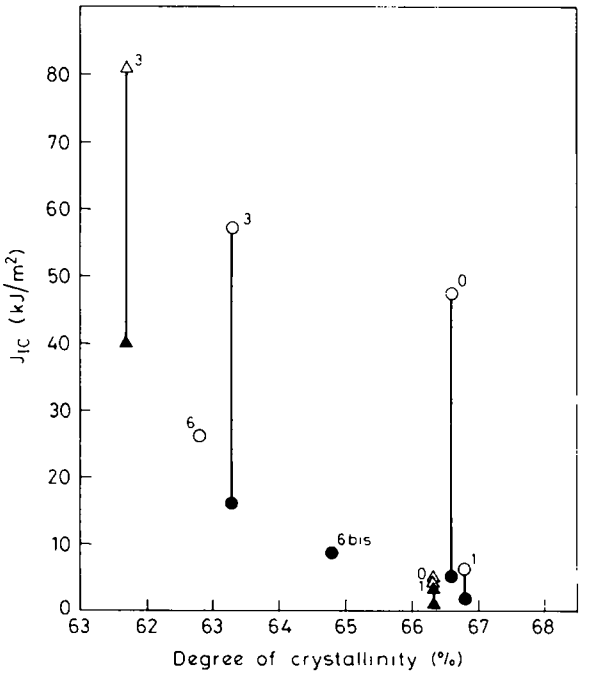

Figure 9 J_{IC} at -60 °C (●, M1; ▲, M2) and 23 °C (○, M1; △, M2). Numbers indicate thermal treatment

Fracture surface analysis was performed, both at small magnification on pictures shot by a reflex camera and with the aid of SEM techniques. Specimens taken from those used to determine J_R curves were examined. As already explained, the specimens were first machine notched, then loaded to propagate the crack to a certain extent, and finally broken at a high rate. In *Figure 3*, all three zones are visible: in the present analysis, the controlled crack advancement zone is the one of interest.

Three different types of fracture surfaces were observed.

Type A (*Figure 3a*) was found at 23°C only; the controlled crack advancement was evidenced by the white paint. This type shows a coarse texture in that zone and a rather irregular crack profile. Thermally treated materials which presented this type of fracture surface (M1-0, M1-2, M1-3, M1-6, M2-2, M2-3) showed a large amount of blunting, with Δa_i generally greater than 1 mm, and high values of J_{IC} and dJ/da (*Table 5*). Two examples of SEM micrographs from type A samples are shown in *Figure 10*, where a stretched texture appears.

Type B (*Figure 3c*) was observed at both −60°C and 23°C; the controlled crack advancement is delimited by a neatly defined front trace. This type shows a smooth texture in that zone. Samples that exhibited this type of behaviour (M1-0, M1-1, M2-0, M2-1 at −60°C, and M1-1, M1-4, M1-5, M2-0, M2-1, M2-7 at 23°C) showed less evident blunting, with Δa_i values generally smaller than 0.2 mm, and lower J_{IC} and dJ/da (*Table 5*). SEM micrographs of type B surfaces (*Figure 11*) are characterized by the same 'tufted' microstructures, with dimples of varying depth and density.

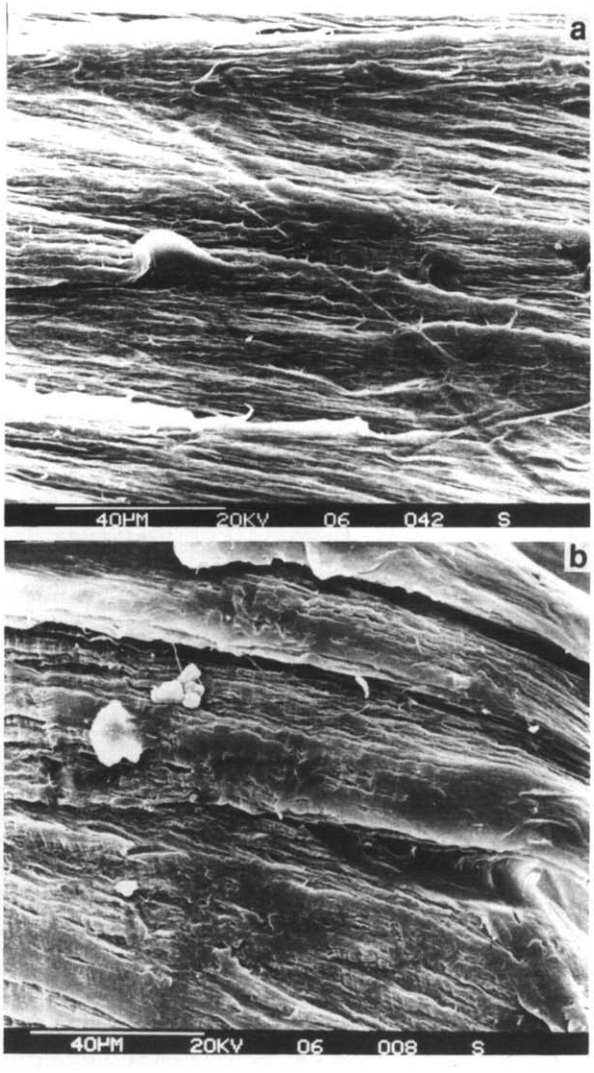

Figure 10 SEM micrographs of type A fracture surface: (a) sample M1-3; (b) sample M1-6, tested at 23 C

Table 5 Results of fracture tests and fractographic analysis

Material and thermal treatment	Test temperature (°C)	Type of fracture surface	J_{IC} (kJ m^{-2})	dJ/da (kJ m^{-3})	Δa_i (mm)
M1-0		B	5.3	2	0.07
M1-1		B	1.9	0.2	0.02
M1-3		C	16	2.5	0.14
M1-6 bis		C	9	1.2	0.28
M1-6 tris		C	14	0.5	0.14
M2-0	−60	B	1.6	1.2	0.04
M2-1		B	1.1	1.3	0.03
M2-3		C	40	2.4	0.6
M2-6 bis		C	28	1.1	0.32
M1-0		A	47.2	11.5	1.37
M1-1		B	6.2	1	0.15
M1-2		A	60	6	1.33
M1-3		A	57	13.3	1.7
M1-4	23	B	6.4	2.6	0.16
M1-5		B	4.3	1	0.11
M1-6		A	26	15.2	0.8
M2-0		B	3.1	0.9	0.1
M2-1		B	4	1.5	0.1
M2-2		A	79	21.6	2.46
M2-3		A	81.1	17.5	2.4
M2-7		B	3.4	0.6	0.09

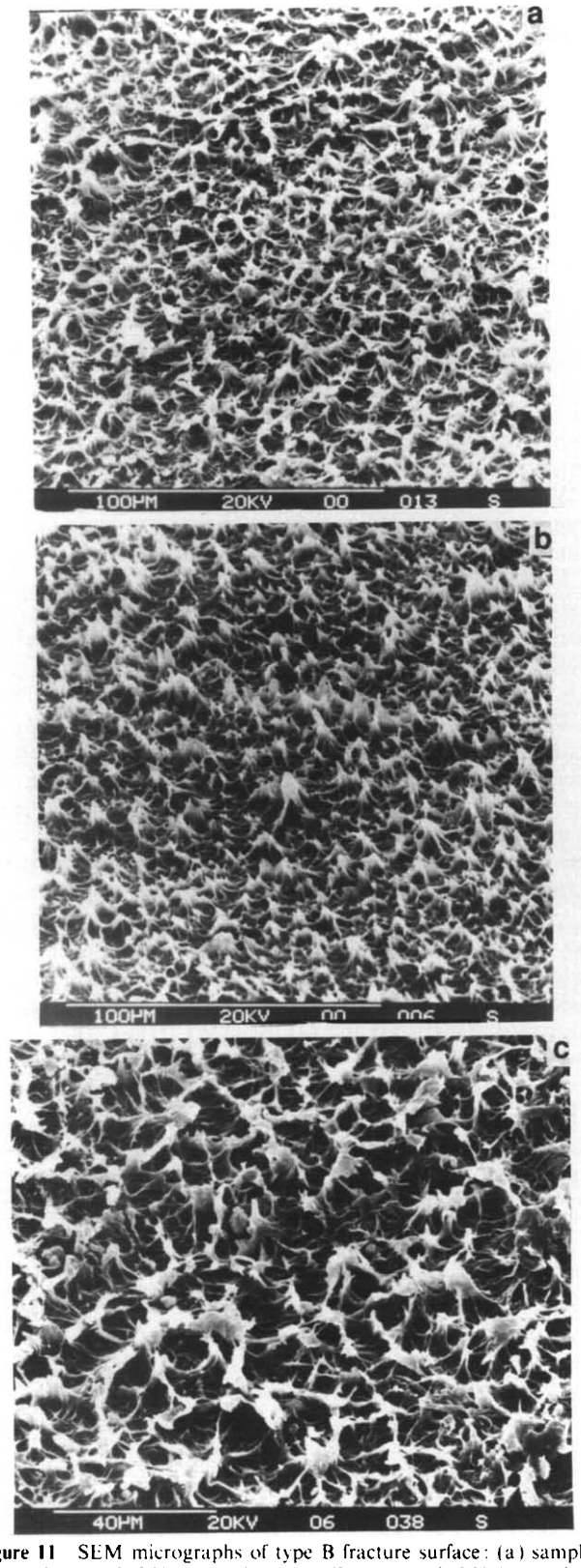

Figure 11 SEM micrographs of type B fracture surface: (a) sample M1-1; (b) sample M1-0, tested at −60 C; (c) sample M1-1, tested at 23 C

Type C (*Figure 3b*) was found at −60 C only, and shows a rough zone immediately ahead of the razor notch identified as the actual crack extension. Samples exhibiting this type of behaviour (M1-3, M1-6, M2-3, M2-6) gave a degree of blunting between that of type A and type B, with Δa_i values ranging from 0.3 to 1.2 mm, and J_{IC} values generally between those of type A and type B (*Table 5*). However, not all specimens grouped as type C show exactly the same fracture surface characteristics; upon closer examination, some differences can be seen (compare, for example, the SEM micrographs shown in *Figure 12*).

In conclusion, the fractographic analysis reveals differences that are reflected in the fracture resistance, J_{IC}: the occurrence of a sharp change in J_{IC} with temperature (*Figure 9*) seems to be related to a change in the fracture surface type.

The results reported so far were all obtained on fracture test specimens 20 mm thick. It should be observed, however, that fracture behaviour, as well as dependence on the type of material, thermal treatment and test temperature, also depends on the stress state as determined by specimen geometry, including specimen thickness. This is evident, for example, from the transition from a type B fracture surface to one more similar to type A which occurred in sample M2-1 on passing from a specimen 20 mm thick to specimens 5 mm thick, cut from the larger specimen. SEM micrographs performed at the same magnification show that the fracture surface microstructure of the 5 mm specimen (*Figure 13b*) is somewhere between type B and type A (*Figures 13a* and *13c*, reproduced from *Figures 11c* and *10b* respectively); tufts appear larger and more stretched than in type B, but shorter than in type A.

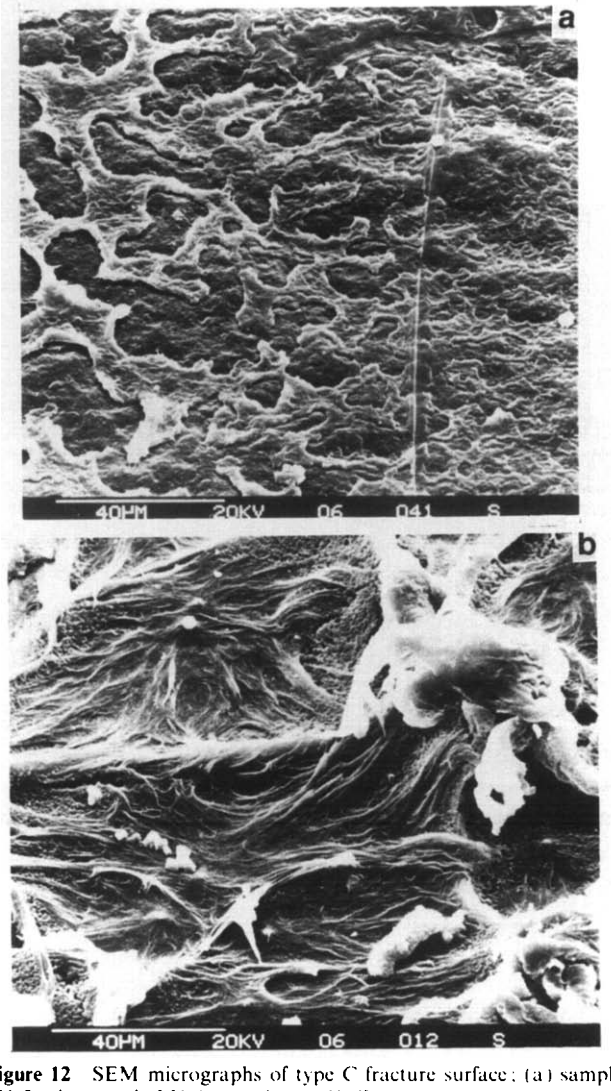

Figure 12 SEM micrographs of type C fracture surface: (a) sample M1-3; (b) sample M1-6, tested at −60 C

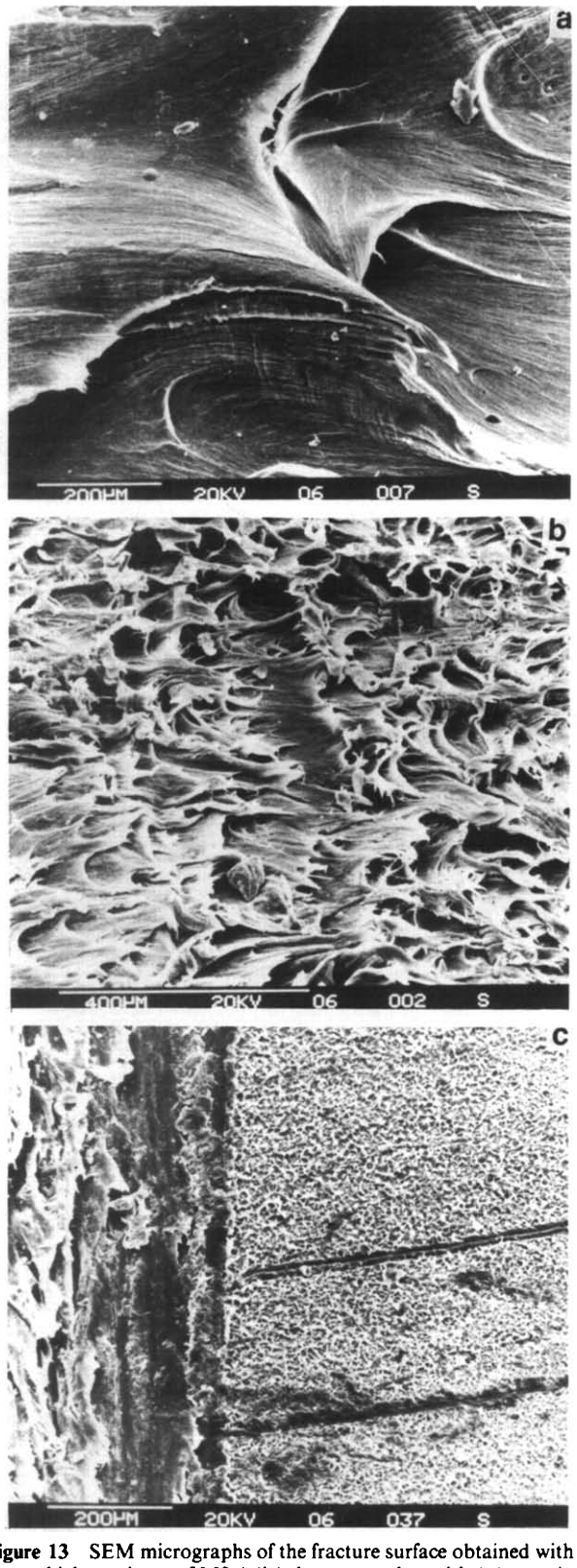

Figure 13 SEM micrographs of the fracture surface obtained with the 5 mm thick specimen of M2-1 (b) shown together with (a) type A and (c) type B fracture surfaces for comparison (see text)

CONCLUSIONS

The fracture behaviour of pipe-grade polyethylenes subjected to various thermal treatments was studied at -60°C and 23°C by the J-integral method. Thermal treatments consisted in slow cooling or quenching from a temperature above melting point down to room temperature, with or without a significant stay at a given intermediate temperature. The main findings of this investigation can be summarized as follows.

Fracture behaviour appears to depend on the type of polyethylene, on structural features that are determined by thermal treatment, and on test temperature. Specifically it was found that a single material may exhibit either tough or brittle behaviour, depending on thermal treatment and test temperature. Obviously, thermal treatment significantly changes some structural features of the material, while variations in test temperature modify the role played by the different structural features in fracture behaviour. On the other hand, it was found that two different polyethylenes may show different fracture behaviour, in spite of the fact that they have been treated in the same way and tested at the same temperature.

We have attempted to correlate two characteristic parameters of fracture behaviour, i.e. toughness at crack initiation, J_{IC}, and crack propagation resistance, dJ/da, with some of the structural parameters of the material. The degree of crystallinity appears to be fairly easy to correlate with the two fracture properties measured at -60°C, but at 23°C no clear correlation is observed, indicating that the degree of crystallinity is not the only structural parameter controlling fracture.

Fractographic analysis was also performed qualitatively. Three types of fracture surfaces which can be briefly classified as coarse (type A), smooth (type B) and intermediate (type C) were observed. Change from one type to another was observed for a given material by changing the thermal treatment or the test temperature. A correspondence was found between variations in J_{IC} and changes in the fracture type when the test temperature passes from -60°C to 23°C. Large J_{IC} variations are associated with transitions in the type of fracture surface from B to A or from B to C, while no change in the type of fracture surface appears when little or no change in the fracture parameters occurs.

Finally, changes in the type of fracture surface were observed on a given thermally treated material, depending on specimen thickness, thus showing the importance of the stress state in fracture behaviour.

These observations underline the complex effects that thermal treatment may have. Evidently, the macroscopic properties of the material are more than simply related to the structural features affected by thermal treatment. Some general effect of thermal treatment on the fracture behaviour of these polyethylenes clearly emerges, however, and, for the technical applications of these materials, the wide variability in performance thus obtainable is of outstanding importance.

ACKNOWLEDGEMENT

The authors are grateful to Professor E. Pedemonte of Genoa University for carrying out SEM analysis of fracture surfaces.

REFERENCES

1 Mandelkern, L. 'Proc. Golden Jubilee Conference on Polyethylenes 1933–1983', London, 8–10 June 1983, Plastics and Rubber Institute, paper D-4 1983
2 Maxfield, J. and Mandelkern, L. *Macromolecules* 1977, **10**, 1141
3 Stack, G. M., Mandelkern, L. and Voigt-Martin, I. G. *Macromolecules* 1984, **17**, 321

4 Mandelkern, L. *Faraday Soc. Disc.* 1979, **68**, 310
5 Norton, D. R. and Keller, A. *J. Mater. Sci.* 1984, **19**, 447
6 Mandelkern, L. and Maxfield, J. *J. Polym. Sci., Polym. Phys. Edn* 1979, **17**, 1913
7 Mandelkern, L., Glotin, M. and Benson, R. A. *Macromolecules* 1987, **14**, 22
8 Stack, G. M., Mandelkern, L. and Voigt-Martin, I. G. *Polym. Bull.* 1982, **8**, 421
9 Voigt-Martin, I. G. and Fischer, E. W. *J. Polym. Sci., Polym. Phys. Edn* 1980, **18**, 2347
10 Grubb, D. T. and Keller, A. *J. Polym. Sci., Polym. Phys. Edn* 1980, **18**, 207
11 Voigt-Martin, I. G. and Mandelkern, L. *J. Polym. Sci., Polym. Phys. Edn* 1984, **22**, 1901
12 Rego Lòpez, J. M. and Gedde, U. W. *Polymer* 1989, **30**, 22
13 Conde Brana, M. T., Iragorri Sainz, J. I., Terseluis, B. and Gedde, U. W. *Polymer* 1989, **30**, 410
14 Ohlberg, S.M. and Roth, J. *J. Appl. Polym. Sci.* 1959, **1** (1), 114
15 Mandell, J. F., Roberts, D. R. and McGarry, F. J. *Polym. Eng. Sci.* 1983, **23** (7), 404
16 Battelle Columbus Laboratory, Annual Report, Gas Research Institute, USA, 1980
17 Lustiger, A. and Markham, R. L. *Polymer* 1983, **24**, 1047
18 Mandelkern, L., Allow, A. L. and Gopolan, M. *J. Phys. Chem.* 1965, **72**, 309
19 Chiang, R. and Flory, P. J. *J. Am. Chem. Soc.* 1961, **83**, 2057
20 Hashemi, S. and Williams, J. G. *Polym. Eng. Sci.* 1986, **26**, 760
21 Rice, J. R., Paris, P. C. and Merkle, J. G. 'Progress in flaw growth and fracture toughness testing', ASTM STP 536, 1973, p. 231
22 Landes, J. D. and Begley, J. A. 'Fracture analysis', ASTM STP 560, 1974, p. 170
23 Chan, M. K. V. and Williams, J. G. *Int. J. Fracture* 1983, **19**, 145
24 Melve, B. *DEng Thesis*, Norwegian Institute of Technology, 1985
25 Turi, E. 'Thermal Characterization of Polymeric Materials', Academic Press, Orlando, 1981, p. 341